Unusual extracellular appendages deployed by the model strain Pseudomonas fluorescens C7R12

Dorian Bergeau, Sylvie Mazurier, Corinne Barbey, Annabelle Mérieau, Andrea Chane, Didier Goux, Sophie Bernard, Azeddine Driouich, Philippe Lemanceau, Maïté Vicré, et al.

PLOS ONE

RESEARCH ARTICLE

Unusual extracellular appendages deployed by the model strain *Pseudomonas fluorescens* C7R12

Dorian Bergeau[1], Sylvie Mazurier[2], Corinne Barbey[1,3], Annabelle Merieau[1,3], Andrea Chane[1], Didier Goux[4], Sophie Bernard[3,5], Azeddine Driouich[3,5], Philippe Lemanceau[2], Maïté Vicré[3,5], Xavier Latour[1,3]*

1 Laboratoire de Microbiologie Signaux et Microenvironnement (LMSM EA 4312)—Normandie Université - LMSM, Evreux, France, **2** Agroécologie, AgroSup Dijon, INRA, Univ. Bourgogne, Univ. Bourgogne Franche-Comté, Dijon, France, **3** Structure Fédérative de Recherche Normandie Végétale 4277 (NORVEGE), Normandie, France, **4** Centre de Microscopie Appliquée à la biologie, SFR 4206 ICORE Université de Caen Normandie (CMAbio3), Caen, France, **5** Laboratoire de Glycobiologie et Matrice Extracellulaire Végétale—Normandie Université - EA 4358 Université de Rouen, Mont-Saint-Aignan, France

* xavier.latour@univ-rouen.fr

Citation: Bergeau D, Mazurier S, Barbey C, Merieau A, Chane A, Goux D, et al. (2019) Unusual extracellular appendages deployed by the model strain *Pseudomonas fluorescens* C7R12. PLoS ONE 14(8): e0221025. https://doi.org/10.1371/journal.pone.0221025

Editor: Fernando Navarro-Garcia, CINVESTAV-IPN, MEXICO

Received: May 31, 2019

Accepted: July 30, 2019

Published: August 28, 2019

Data Availability Statement: All relevant data are within the paper and its Supporting Information files.

Funding: This research was supported by grants from French institutions (Ministère de l'Enseignement Supérieur, de la Recherche et de l'innovation, Région Normandie & the Evreux Portes de Normandie agglomération), the VASI (Végétal-Agronomie-Sols-Innovation) network & FEDER (European Union). The funders had no role in study design, data collection and analysis,

Abstract

Pseudomonas fluorescens is considered to be a typical plant-associated saprophytic bacterium with no pathogenic potential. Indeed, some *P. fluorescens* strains are well-known rhizobacteria that promote plant growth by direct stimulation, by preventing the deleterious effects of pathogens, or both. *Pseudomonas fluorescens* C7R12 is a rhizosphere-competent strain that is effective as a biocontrol agent and promotes plant growth and arbuscular mycorrhization. This strain has been studied in detail, but no visual evidence has ever been obtained for extracellular structures potentially involved in its remarkable fitness and biocontrol performances. On transmission electron microscopy of negatively stained C7R12 cells, we observed the following appendages: multiple polar flagella, an inducible putative type three secretion system typical of phytopathogenic *Pseudomonas syringae* strains and densely bundled fimbria-like appendages forming a broad fractal-like dendritic network around single cells and microcolonies. The deployment of one or other of these elements on the bacterial surface depends on the composition and affinity for the water of the microenvironment. The existence, within this single strain, of machineries known to be involved in motility, chemotaxis, hypersensitive response, cellular adhesion and biofilm formation, may partly explain the strong interactions of strain C7R12 with plants and associated microflora in addition to the type three secretion system previously shown to be implied in mycorrhizae promotion.

Introduction

Fluorescent pseudomonads are so-named because they produce soluble greenish pigments in conditions of iron limitation that fluoresce when illuminated with UV light [1]. These

decision to publish, or preparation of the manuscript.

Competing interests: The authors have declared that no competing interests exist.

ubiquitous γ-proteobacteria have a considerable potential for adaptation to fluctuating environmental conditions, thanks to their highly versatile metabolism and the plasticity of their large genome [2–6]. This group of bacteria includes the species *Pseudomonas fluorescens*, which is generally considered to be a saprophytic rhizobacterium because its densities (10^6 to 10^8 CFU/g root) and metabolic activities are increased in the plant rhizosphere [7–10]. In addition, some strains protect plants from infection by interfering with phytopathogenic agents. This biocontrol activity generally involves competition with pathogens for space and/or nutrients, antagonism *via* the synthesis of toxic agents, antibiotics and biosurfactants, and stimulation of plant defenses [11–15]. The location and fitness of *P. fluorescens* render this antagonistic species even more powerful for treating diseases of roots and tubers, which are not generally accessible to germicidal treatments [16,17].

It is now widely accepted that the strong plant colonization and biocontrol capacities of fluorescent pseudomonads are associated with cell motility and chemotaxis towards the rhizosphere in addition to cell adhesion and biofilm formation on the roots [18–22]. These physical plant-bacterium interactions are closely associated with the presence of bacterial extracellular structures, such as flagella, fimbriae, pili and secretion systems [23–27]. Unfortunately, these nanostructures are only clearly visible on electron microscopy (EM), and they are therefore generally detected indirectly. Indeed, the presence of flagella, fimbriae and pili, which are involved in swimming, swarming and twitching motilities, respectively, is deduced from observations of bacterial growth on appropriate agar plates [24,28]. Likewise, evidence for the presence of a functional type three secretion system (T3SS) is provided by the observation of a hypersensitive response (HR) in tobacco leaves 24 to 48 hours after the infiltration of the bacterium concerned [29–31]. The difficulties encountered in observations of extracellular appendages result from their extremely small size (in the nanometer range) and brittleness: these delicate structures are generally destroyed by shaking during culture or during the transfer of cells onto the support for microscopic observation. Moreover, little is known about the environmental conditions triggering the synthesis of these components [32,33].

We performed ultrastructural observations by transmission electron microscopy (TEM). We observed several different membrane machineries on the rhizosphere-competent biocontrol strain *P. fluorescens* C7R12. This model strain harbors a remarkable set of extracellular structures, including a polar bundle of flagella, a putative T3SS that seems to be synthesized in response to fructose or trehalose induction, and bundles of dendritic fibrils forming a huge network of cells and microcolonies. We discuss the putative role of these structures in the primary steps of adhesion and biofilm formation.

Materials and methods

Bacterial strains and culture conditions

Pseudomonas fluorescens C7R12 [34] and a T3SS$^-$ mutant derived from it, C7SM7, were used for these experiments. *Pseudomonas fluorescens* C7SM7 was obtained by site-directed mutagenesis of *hrc*C, a gene encoding an outer membrane pore forming protein required for type III-mediated secretion [35]. This mutant has been chosen since HrcC is required for the secretion of the HrpA protein forming the pilus of T3SSs belonging to the Hrp1 family [36]. Bacterial cells were cultured at 25˚C in King's B medium [37], a glycerol-rich medium with a low iron content that induces the synthesis of *Pseudomonas* siderophores and secondary metabolites [1,12], or in an *hrp*-inducing minimal medium (HIM) as described by Huynh et al. [38] and with the following composition: 1.7 mM NaCl, 1.7 mM $MgCl_2$, 7.6 mM $(NH_4)_2SO_4$, 50 mM KH_2PO_4, pH 5.7, supplemented with 10 mM glucose, fructose, sucrose or trehalose as the sole carbon source. For induction of the T3SS *hrp*A model gene, bacteria were first cultured in

liquid KB medium to an OD at 600 nm of 0.6–0.8. The bacteria were washed twice in 10 mM $MgCl_2$ and the OD_{600} was adjusted to 0.6 in liquid HIM. Induction was performed at 25˚C, with shaking (180 rpm). KB medium was used to repress T3SS (i.e. as a non-inducing medium), to establish the basal level of *hrp*A gene expression (control).

Swimming, swarming and twitching motility assays

Motility assays were performed on KB medium supplemented with 0.3%, 0.6% or 1% agar, for swimming, swarming and twitching motilities, respectively as previously described [39]. Briefly, swimming motility assay plates were inoculated with a toothpick. Swarming motility assay plates were inoculated by the deposition of 5 μl of overnight bacterial culture on the surface of the medium. Twitching motility assay plates were inoculated by depositing 5 μl of overnight bacterial culture underneath the medium, at the bottom of the Petri dish. The plates were incubated at 25˚C for 48 h. Motility was assessed by measuring mean dendrite length for swarming, or the total diameter of the circular turbid zone for swimming. Twitching motility was assessed by determining the diameter of growth at the interface between the agar and the bottom of the Petri dish. This was achieved by removing the agar, washing the unattached cells of the plate with water, and staining the cells attached to the plate with crystal violet (1% [wt/vol] solution).

Total RNA extraction and cDNA synthesis

Total RNA was extracted from 10^9 bacteria by the hot acid-phenol method [40]. As required, a volume of culture containing 10^9 bacteria was sampled and mixed with an equal volume of 100% ethanol 100% to stop transcription. Bacterial cultures were centrifuged at 4 000 × *g* for 10 min and the bacterial pellet was resuspended in 300 μl of lysis buffer (0.02 M sodium acetate, pH 5.5, 0.5% (w/v) SDS, 1 mM EDTA). Total RNA was then isolated by two rounds of extraction in 600 μl of hot acid phenol for three minutes each (pH 4.3; 60˚C). The mixture was centrifuged at 13 000 × *g* for 15 min, and the aqueous phase was treated with 500 μl chloroform/isoamyl alcohol (24:1) and centrifuged as previously described. Total RNA was precipitated by overnight incubation of the supernatant at -20˚C with two volumes of 100% ethanol containing 100 mM sodium acetate. The precipitated RNA was collected by centrifugation. The pellet was washed in 75% ethanol and resuspended in 50 μl DEPC water and treated with Ambion TURBO DNase (Life Technologies) for 2 h at 37˚C. We checked for the absence of DNA contaminants by PCR with the standard NEB kit, using the 16S-FOR/16S-REV primers (**S1 Table**). Total RNA was converted into cDNA by reverse transcription with the High-capacity cDNA RT Kit (Applied Biosystem).

Quantitative RT-PCR

Specific primers for the target genes *hrp*A, and the 16S rRNA gene of *P. fluorescens* C7R12 were designed with Primer Express Software v3.0.1 (**S1 Table**). Real-time quantitative amplification was performed with the 7500 Fast Real Time PCR system (Applied Biosystems). Reactions were performed in a 13 μl mixture containing 6.5 μl SYBR Green PCR Master Mix (2X SYBR Green 1 Dye, AmpliTaq Gold DNA Polymerase, dNTPs with dUTPs) with each primer present at a final concentration of 0.2 μM and 7.5 ng cDNA. The thermal cycling program was as follows: 95˚C for 20 s, followed by 40 cycles of 95˚C for 10 s, 60˚C for 30 s and 72˚C for 6 s, and then 95˚C for 15 s, 60˚C for 1 min and 95˚C for 15 s. We used 16S rRNA as an internal control and the standard deviation in each case was below the 0.15 threshold cycle (CT). Relative quantification was performed as previously described, by the comparative CT ($-2^{\Delta\Delta CT}$) method [41].

Preparation of samples for transmission electron microscopy

Bacteria were visualized on 200-mesh nickel EM grids (mesh diameter of 74 μm) coated with 2% Formvar (Leica Microsystems), a polyvinyl formal resin formed by polyvinyl alcohol and formaldehyde copolymerization with polyvinyl acetate, and produced by Monsanto Chemical Company (St. Louis, Missouri).

For the observation of flagella and the T3SS, assay conditions inducing the formation of these structures and preserving their integrity were established with a modified version of the protocol described by Roine et al. [42]. Bacteria were grown on solid KB or HMI medium supplemented with 10 mM fructose or trehalose as the sole carbon source, at 25˚C for 48 h. The EM grids were then coated with the bacteria by transfer from the agar plate. The formvar-coated side of the grid was placed in contact with the bacterial lawn for 10 min to obtain a footprint of the cells and the organelles synthesized on the corresponding agar medium. For the observation of pili and dendritic fibril bundles, assays were performed according to an original protocol in which bacteria were cultured directly in liquid HIM on grids. The bacteria were first cultured overnight in KB medium. They were washed twice in 1 mM $MgCl_2$, resuspended in HIM and the OD_{600} was adjusted to 10^8 CFU/ml. A 20 μl droplet of this suspension was deposited in the center of a 9-cm Petri dish lined with wet filter paper. The EM grid was placed on the drop and the Petri dish was sealed with Parafilm. The plates containing the grids were incubated in a growth chamber at 25˚C, in a saturated atmosphere, for 8, 12, 24 and 48 h.

Once the bacteria were loaded onto the grids, they were fixed by transferring the grids for 30 min onto a 20 μl drop containing 2% paraformaldehyde and 0.5% glutaraldehyde in PBS (pH 7.2, 137 mM NaCl, 2.7 mM KCl, 10 mM Na_2HPO_4 and 1.76 mM KH_2PO_4). Grids were then washed three times, for 5 minutes each, by placing them on a 50 μl drop of PBS and three times, for 5 minutes each, by placing them on a 50 μl drop of distilled water. The washed specimens were negatively stained by incubation for 10 s in 1% phosphotungstic acid, the pH of which was adjusted to pH 6.5 with KOH, and the specimens were then allowed to dry in air before viewing.

Transmission electron microscopy

All observations were performed at PRIMACEN, the Normandy Cell Imaging Platform (Mont-Saint-Aignan, France), and/or at CMABio, the Center for Microscopy Applied to Biology (Caen, France) of Normandy University. Observations were performed on Tecnai 12 Bio-Twin (PRIMACEN) or JEO1 1011 (CMABio3) transmission electron microscopes operating at 80 kV. Images were acquired with an Erlangshen 500W (PRIMACEN) or Gatan Orius 200 (CMABio3) camera, and processed with Gatan Digital Micrograph software (on both microscopes).

Statistical analyses

Cultures were set up in triplicate from three independent cultures, each of which was set up from an independent preculture. For quantitative PCR, we tested the null hypothesis that each expression value was not significantly different from the other expression values (*P* value calculated). *P* values below 0.05 were considered significant (*, $P < 0.05$). The standard deviation was below 0.15 *Ct* units. The results presented are the mean values from at least three independent experiments. Statistical analysis was performed with DataAssistTM software (v3.01), for the relative quantification of gene expression according to the comparative CT (2–ΔΔCT) method [41].

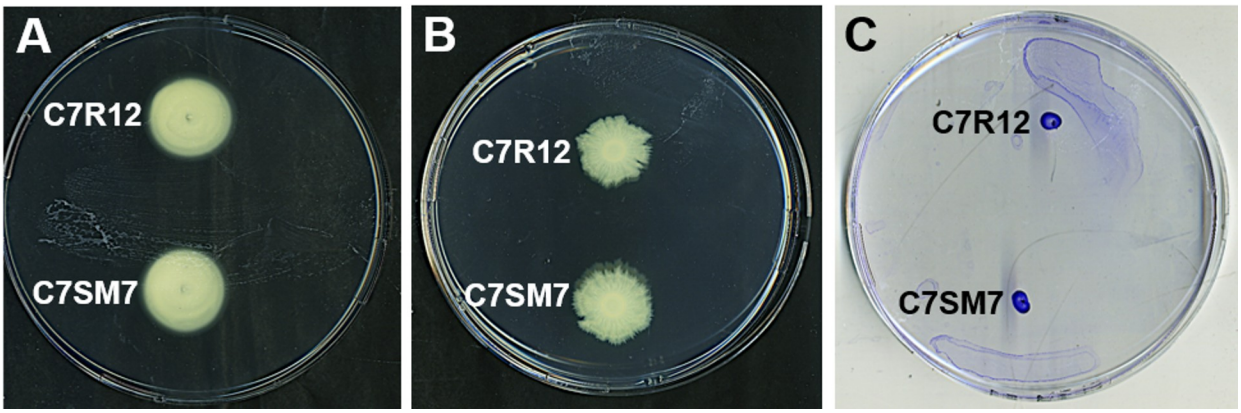

Fig 1. Swimming and swarming motilities of *P. fluorescens* C7R12 and a T3SS-negative mutant strain derived from it (C7SM7 strain). Cells were used to inoculate swimming (A), swarming (B) or twitching (C) motility assay agar plates containing King's B medium, which were scanned after 48 h of incubation at 25˚C. The results shown are representative of three independent experiments, each performed at least in triplicate.

https://doi.org/10.1371/journal.pone.0221025.g001

Results

Motilities and lophotrichous flagellation of *Pseudomonas fluorescens* C7R12

Flagella are used in both swimming motility in liquids and swarming motility on wet semi-solid surfaces [43]. *Pseudomonas fluorescens* C7R12 strain and the T3SS-defective mutant derived from it, C7SM7, both displayed swimming (**Fig 1A**) and swarming (**Fig 1B**) motilities in KB agar. For swimming, the mean of the diameter of the turbid zone was similar for the two strains (27.4 ± 1.3 mm for the C7R12 strain and 28 ± 1.3 mm for the C7SM7 strain). In the most studies of *Pseudomonas aeruginosa*, a flagellum with a polar insertion is responsible for this mode of motility and is generally observed in aqueous environments [44]. Unlike swimming, swarming motility requires a concerted multicellular effort, biosurfactant secretion to decrease the surface tension of the swarm fluid and, in some cases, an increase in the number of flagella [45]. Swarming appears to be a mode of motility enabling bacterial populations to colonize surfaces rapidly, resulting in biofilm formation [43]. The C7R12 and C7SM7 strains were able to migrate away from the initial location collectively, with a mean growth diameter of 32.2 ± 2 mm measured for C7R12, and of 31.9 ± 3.1 mm for C7SM7, in our KB agar conditions. The swarming observed took the form of small fringes (**Fig 1B**) as previously described for other *P. fluorescens* strains [46]. However, this swarming did not result in the formation of the expanding irregular branching pattern typical of swarming motility in *P. aeruginosa*, as described by Rashid and Kornberg [47].

Twitching motility is a mode of translocation over semi-solid or solid surfaces in humid conditions. It is dependent on the presence of retractile type IV pili, but does not require flagella [48]. In twitching motility, translocation across the surface is mediated by the extension and retraction of pili and corresponds to a collective behavior supporting colony expansion [48]. In our twitching motility assays, both strains formed a dense crystal violet-stained spot, the diameter of which corresponded to that of the initial inoculum (5 μl) (**Fig 1C**). Thus, these strains were unable to move over the surface of the Petri dish, but they were able to adhere to it. We can therefore conclude that these *P. fluorescens* strains have no twitching motility and probably do not produce type IV pili under our experimental conditions.

We investigated the type of cilia responsible for the swimming and swarming of the C7R12 strain, by culturing this strain on KB agar plates and then transferring it to an EM grid. Cells

were negatively stained and examined by high-resolution TEM. *P. fluorescens* C7R12 was rod-shaped, about 2 μm long and usually covered with four to seven flagella all connected to the cell body at the same polar position (**Fig 2A and 2B**). In our assay conditions, these flagella were about 4 to 5 μm long and had a diameter of about 20 nm. In some bacteria, the base of the multiple flagella is surrounded by a specialized region of the cell membrane known as the polar organelle [49]. No such polar organelle was observed here (**Fig 2C**). The multiple flagella are thought to act in concert to drive bacterial swimming by pushing, pulling or coiling around the cell body in the vicinity of a semi-solid agar surface [50], consistent with our findings (**Fig 1**).

The expression of *hrp*A, encoding the main protein of the T3SS pilus, is strongly induced by fructose, sucrose and trehalose in minimal medium

The T3SS apparatus is not constitutively produced by bacteria and remains difficult to observe without specific and favorable assay conditions [33,51]. Various culture media favoring the production of T3SS in the phytopathogen *Pseudomonas syringae* have been described. We chose to use a basal salt medium mimicking the composition and pH of the plant apoplast [38,52]. These conditions are thought to trigger the production, by bacteria, of a T3SS injectisome close to the potential target (i.e. plant cells) [32,38,53]. We added various plant sugars to this minimal medium, and compared their ability to act as a carbon source and to induce the production of the T3SS by the *P. fluorescens* C7R12 strain.

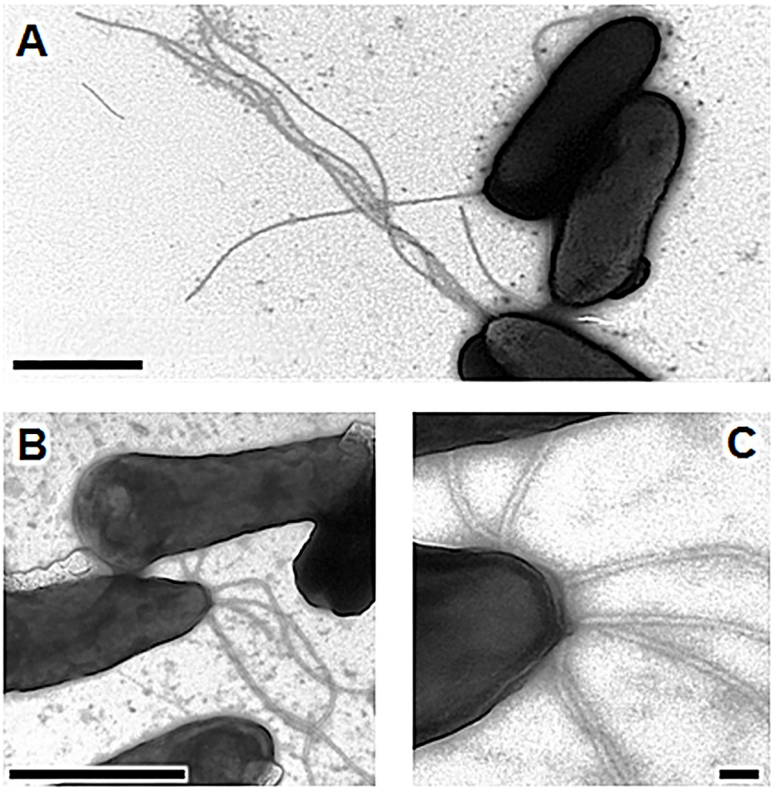

Fig 2. Production of flagella by *P. fluorescens* C7R12. Cells were grown for 48 h at 25˚C on plates containing solidified King's B medium. They were then transferred by footprint to the electron microscopy grids and negatively stained with phosphotungstic acid. The cells harbored a lophotrichous cilium, generally composed of multiple long flagella (A). Up to seven flagella were observed emerging from a single bacterium, as shown in (B). An enlargement of this image reveals polar insertion details and can be used to estimate the diameter of each pilus (C); the sizes of the scale bars are 1 μm (A,B) and 0.1 μm (C).

https://doi.org/10.1371/journal.pone.0221025.g002

We assessed the efficacy of this medium for inducing T3SS by first evaluating the relative expression level of a key T3SS gene, *hrp*A, which is known to be highly expressed and representative of HrpL-regulated T3SS genes in *P. syringae* [32,33]. This gene encodes the major structural protein of the T3SS pilus, enabling the pilus to elongate until it reaches its target, through polymerization [54]. RT-qPCR analysis was performed to compare *hrp*A expression between the C7R12 strain cultured in liquid HIM medium and in KB medium. With glucose as the inducer, *hrp*A transcription levels in HIM were significantly higher than those observed in KB cultures, with a maximum 50-fold difference after 2 h of incubation (**Fig 3A**). Higher fold-changes were obtained for media containing fructose, sucrose or trehalose in place of glucose. Fructose and sucrose induced a maximum fold-change of about 180 after 6 h of incubation (**Fig 3B and 3C**). The similarity of the transcription levels obtained with these two sugars may be explained by the composition of sucrose, a disaccharide with fructose as one of its components. Interestingly, stronger *hrp*A induction (around 220-fold) occurred when the C7R12 strain was cultured in HIM supplemented with trehalose (**Fig 3D**). We therefore chose to use HIM supplemented with fructose or trehalose for subsequent TEM studies.

Occurrence and architecture of type III secretion systems

The induction of HR, a form of localized programmed plant cell death at the site of infection, suggests that effector proteins are translocated into the plant cell via a T3SS [29–31]. A HR can

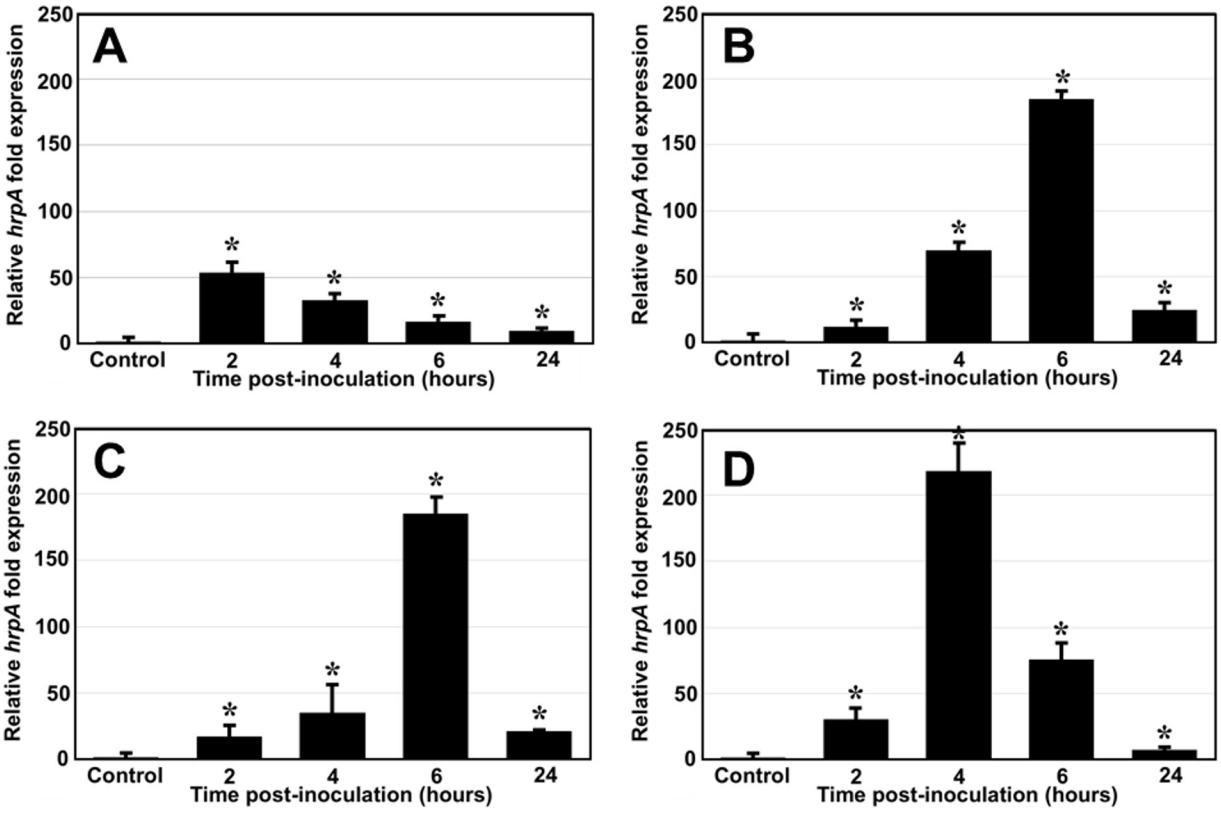

Fig 3. Induction of *hrpA* expression in *P. fluorescens* C7R12 cultured in HIM supplemented with mono- or disaccharides. We analyzed *hrp*A transcription by RT-qPCR on the *P. fluorescens* C7R12 strain grown at 25˚C in *hrp*-inducting minimal medium supplemented with 10 mM glucose (A), fructose (B), sucrose (C) or trehalose (D). Levels of *hrp*A expression are expressed relative to those obtained on King B (non-inducing) rich medium. The data shown are the mean values obtained in three independent experiments. Statistical analysis was performed with DataAssistTM software (v3.01), with relative gene expression levels quantified by the comparative CT ($2^{-\Delta\Delta CT}$) method. The significances of differences between mean values were determined by calculating *p*-values in Student's *t* tests ($^{*}P < 0.05$).

https://doi.org/10.1371/journal.pone.0221025.g003

be generated only if the bacterium harbors an operational T3SS and injects effector proteins into the plant cell [55–57]. *P. fluorescens* is considered to be a "safe" saprophytic rhizobacterial species with no phytopathogenic potential [3,4]. It does not, therefore usually elicit a HR [58]. C7R12 differs from most *P. fluorescens* strains in its ability to elicit a HR similar to that recorded with *P. syringae* pv. tomato DC3000 on tobacco leaves within 24 hours, and the presence of T3SS gene sequences very similar to those present in this reference strain [35,59]. By contrast, the T3SS mutant C7SM7 was unable to so induce a HR, indicating that the HrcC structural protein targeted during the construction of this mutant is an indispensable element of the architecture of the T3SS [35]. We therefore used the C7SM7 strain as a negative control with no T3SS appendage.

The T3SS manufactured by *P. syringae* phytopathogens belong to the Hrp1 family [60]. They form long thin filaments that may extend from 200 nm to several micrometers in length, with a diameter of 10–12 nm, in laboratory conditions [54]. The TEM micrographs obtained in our assay conditions revealed putative T3SS appendages of about 700 to 1,750 nm in length, with a diameter of about 10 nm. Unlike the polar flagella, the T3SS pili were always positioned on the elongated part of the cell body **(Fig 4A)**. In this context, we also observed the basal portion of the pilus inserted into the outer membrane, which formed a ring (presumed to be the HrcC hexamer) from which the pilus extended **(Fig 4B),** as already reported for *P. syringae* DC3000 [53]. As expected, we observed no such structures in the C7SM7 *hrc*C^{-} mutant (**Fig 4C**). Thus, *P. fluorescens* C7R12 produces an extracellular apparatus similar to those of Hrp1-T3SS family, as visualized in *P. syringae* DC3000 [42,53,61]. This finding is entirely consistent with the previous Hrp1-like classification of the *hrc/hrp* gene cluster in the C7R12 genome [59,62].

Deployment of a network of dendritic fibril bundles

Most TEM specimens must be supported on a thin electron-transparent film, to hold the sample in place. Formvar films are thermoplastic resins composed of polyvinyl formals. They are a frequent choice of film grid for TEM because they allow the use of grids with a lower mesh rating (see Materials and Methods section). When the C7R12 and C7SM7 strains were cultured directly in a drop of HIM placed on the surface of an abiotic formvar grid, the cells rapidly deployed novel extracellular structures. We observed long, thick pili associated to various extents into fibrils, which eventually formed fibril bundles, depending on growth stage. After 8 hours of culture, fibrils seemed to be synthesized by microcolonies consisting of a few individual cells to several dozen cells. These fibrils seemed to pack the bacterial wall or the border of the whole colony, forming a fibrous capsule connecting individuals or microcolonies to each other **(Fig 5A and 5B)**. In rare cases, the fibrils appeared to be produced by and collected around a single cell. However, we never clearly observed a pilus or fibril anchored in the cell membrane or localized to a particular part of the cell, such as the pole, and we were unable to detect potential sites of insertion into the cell (**Fig 5C**). One possible reason for this is that *P. fluorescens* cells release their pili proteins or components into the extracellular compartment in order for binding to the fibrils to lengthen them.

After 24 hours, microcolonies including a few hundred individuals were able to deploy a fractal network of fibril bundles over an area of up to about a 1000 μm^2 **(Fig 6A)**. The bundled fibrils seemed to be closely associated with microcolony structures. Each fibril consisted of large parallel arrays of two to eight thin packed individual pili with diameters of about 10–15 nm. The extremities of each bundle displayed branched dendritic growth and subdivision, optimizing the exploration and colonization of the contact surface **(Fig 6A and 6B)**. At this stage, individual pili were rarely observed in the fibrils, except at the growing extremities of the

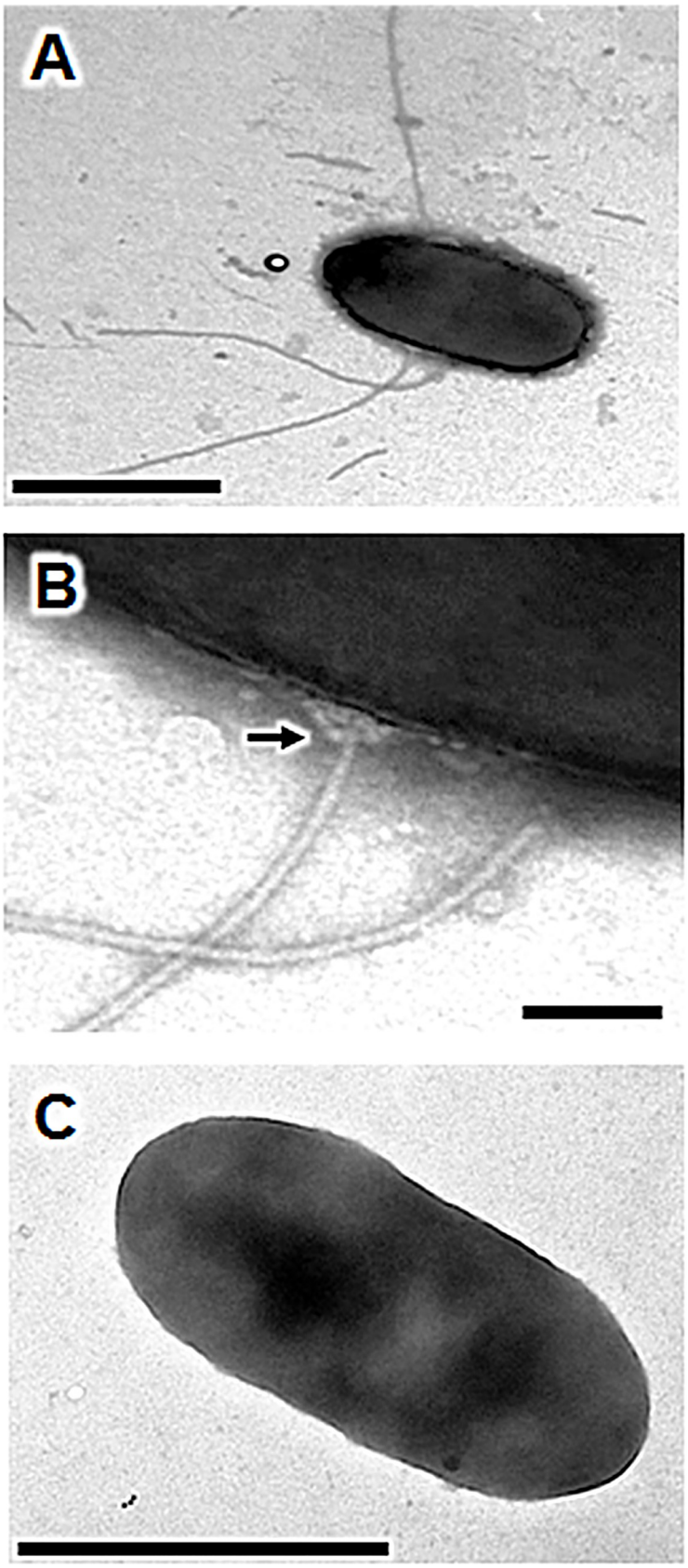
A
B
C

Fig 4. Production of a type three secretion system (T3SS) by *P. fluorescens* C7R12. Cells were grown for 48 h at 25˚C on solidified *hrp*-inducing minimal medium supplemented with fructose (10 mM). They were then transferred by footprint to the electron microscopy grids. Transmission electron micrographs of negatively stained *P. fluorescens* C7R12 cells showing (A) three non-polar long and thin putative Hrp pili. (B) A magnification of the image in A shows the presumed T3SS basal body (black arrow) embedded in the outer membrane of this Gram-negative bacterium; (C) Under these assay conditions, the T3SS-negative mutant C7SM7, used as negative control, is deprived of appendages; the sizes of scale bars are 1 μm (A,C) and 0.1 μm (B).

https://doi.org/10.1371/journal.pone.0221025.g004

bundle (**Fig 6B and 6C**). After 48 hours, the bundles of fibrils appeared darker on TEM, as they had become larger and denser (**Fig 6D**). An analysis of high-magnification images of a single fibril revealed a regular structure resembling the stacking of several dozens of pilus subunits (**Fig 6E**).

Discussion

Pseudomonas fluorescens C7R12 is a strain isolated from a soil naturally suppressive to Fusarium wilt. It has been shown to be an effective biocontrol agent [62,63], to protect *Medicago truncatula* against *Pythium* [35], to promote plant growth and arbuscular mycorrhization [35,64,65], and to colonize the rhizosphere and the root tissues of various plant species efficiently [34,64,66]. These abilities have been shown to be associated with (*i*) the presence of a functional primary metabolism coupling aerobic and nitrogen oxide respiration [67,68], (*ii*) an ability to scavenge efficiently from the environment [34], (*iii*) a capacity to synthesize a siderophore (pyoverdine) with a very high affinity for iron and an ability to improve plant iron nutrition [69–71], (*iv*) the presence of a functional T3SS [35], and (*v*) an ability to assimilate specific compounds from fungi and plants (e.g. sucrose, trehalose) [9,72]. By contrast, the ability of *P. fluorescens* C7R12 to move, adhere to the root surface, or develop physical interactions with root cells or microbial partners (e.g. mycorrhizae) in the rhizosphere has yet to be evaluated, and the existence of extracellular appendages potentially involved in these behaviors has not been investigated.

The bacterial flagellum is an apparatus composed of more than 20 different proteins, with a basal body that crosses the cell wall and is connected to the flagellar filament by a hook, serving

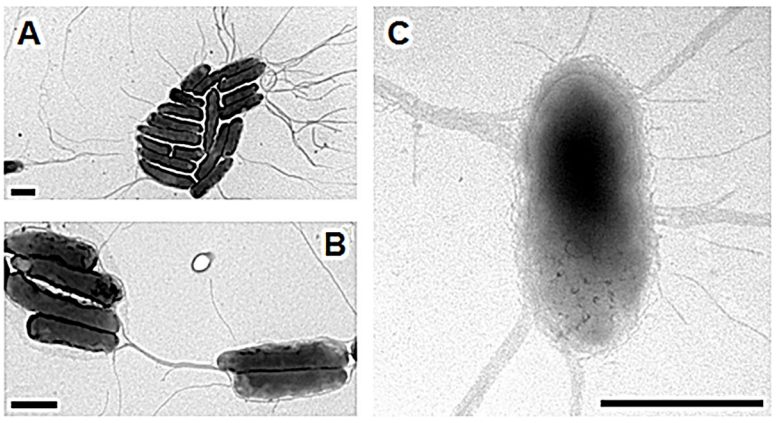

Fig 5. Production of pili and fibrils by *P. fluorescens* C7R12 and its T3SS-negative mutant C7SM7. Cells were grown at 25˚C on formvar electron microscopy grids on a drop of *hrp*-inducing minimal medium supplemented with fructose or trehalose (10 mM). Transmission electron micrographs of negatively stained *P. fluorescens* C7R12 (A) and its *hrc*C$^-$ mutant C7SM7 (B) microcolonies or single cells (C). *P. fluorescens* C7R12 and the T3SS mutant C7SM7 produced similar fibrils from 8 h of incubation onwards. These fibrils encircled both single cells (C) and microcolonies (A,B) and connected them (B); the size of the scale bars is 1 μm.

https://doi.org/10.1371/journal.pone.0221025.g005

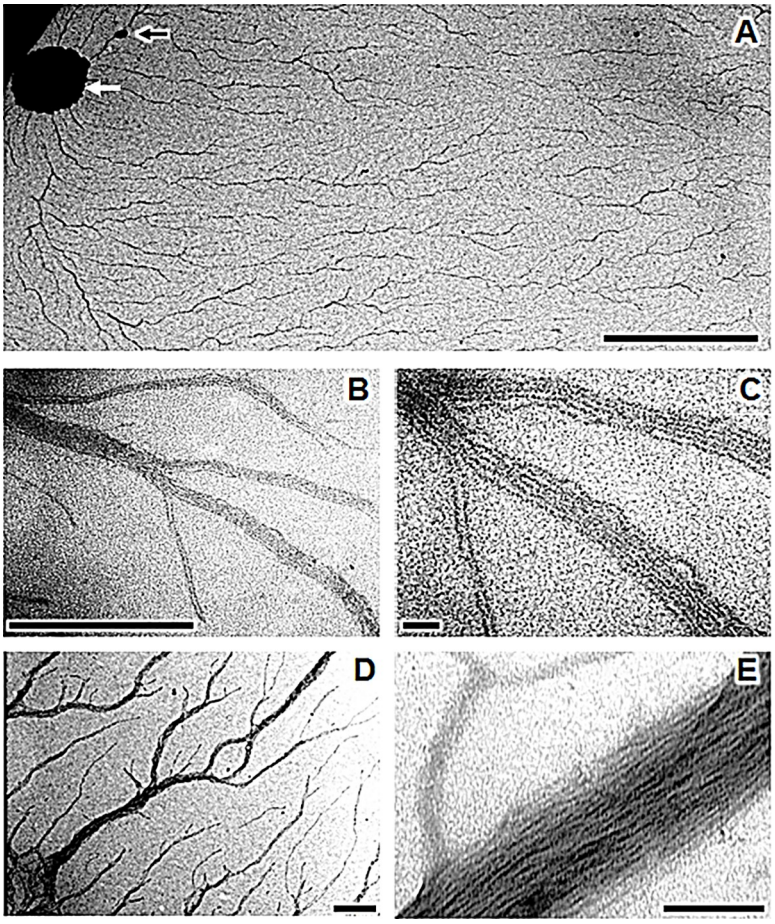

Fig 6. Fibril bundle network deployed by *P. fluorescens* C7R12. Cells were grown at 25˚C on formvar electron microscopy grids on a drop of *hrp*-inductive minimal medium supplemented with fructose (10 mM). (A) Extended dendritic network of fibrils produced by a microcolony of about a hundred cells (black arrow) and a single cell (white arrow) after 24 h. (B) Apex of a fibril with its extension fork. (C) A magnification of the image in B showing the detailed structure of fibrils composed of one to five contiguous pili. (D) Dense fibril bundles obtained after 48 h. (E) A magnification of the image in D showing the ramification of a bundle composed of several dozen fibrils; the sizes of the scale bars are 10 μm (A), 1 μm (B,D), and 0.1 μm (C,E).

https://doi.org/10.1371/journal.pone.0221025.g006

as a flexible joint to change the angle of flagellar rotation [25,73]. It is an effective locomotion organelle that enables bacteria to achieve speeds exceeding many cell body lengths per second [74]. Flagella have also been reported to function as adhesins, playing a key role in bacterial adhesion and virulence [25]. Members of the species *P. fluorescens* have traditionally been considered to have a single flagellum at one of the cell poles, the so-called "monotrichous" conformation [22,75,76]. However, cells of *P. fluorescens* C7R12 have an unusual lophotrichous ciliature, with a polar tuft of four to seven flagella. Bacterial motility plays a key role in dispersion and surface colonization in soil-resident bacteria, such as *P. fluorescens* [19,77]. This motility is dependent on the number of flagella and their arrangement on the cell body [78]. Hintsche et al. [50] showed that a *Pseudomonas putida* strain with a polar tuft of helical flagella could use different swimming patterns, with the bacteria able to move as "pushers" or "pullers" or to propel themselves with the bundle of flagella wrapped around the cell body. The strong rhizosphere-competence of the C7R12 strain may, thus, be at least partly due to the presence of this atypical multiple flagellation, increasing the speed of movement (hypermotility), and

altering the nature of displacements (**Fig 1**), thereby increasing fitness and chemotaxis capacity in the vicinity of plants [75,79]. However, unanswered questions remain about the role of this unusual flagellation in the adhesion process.

Type three secretion systems have been shown to play a determining role in host interactions mediated by fluorescent pseudomonads, including the opportunistic pathogen of animals and humans *Pseudomonas aeruginosa* and the plant pathogen *Pseudomonas syringae* [80,81]. In these pathogenic species of *Pseudomonas*, the T3SS is involved in cell-to-cell contact with the eukaryotic host and in bacterial virulence. Genes encoding the basic structural elements of the T3SS are conserved among Gram-negative bacteria [60,82]. Eight families of T3SSs have been described on the basis of sequence analyses [83,84]. The T3SS of *P. aeruginosa* involved in bacterial virulence belongs to the Ysc-T3SS family. It forms a short needle-like structure that acts as an injectisome, delivering toxins to the target cell cytosol [85,86]. The T3SS of *P. syringae*, which has been implicated in plant pathogenicity, belongs to the Hrp1-T3SS family. It forms a long, thin, flexible pilus, capable of penetrating the thick walls of plant cells. This pilus is essential for the injection of multiple effector proteins into plant cells to suppress plant innate immune defenses, manipulate hormone signaling and trigger cell death [30,57,80,87]. *P. fluorescens* is considered to be non-phytopathogenic, but the presence of T3SS genes related to those of the Hrp1-T3SS family has been reported in some rhizosphere isolates [83,88–94]. However, only a minority of these strains can trigger a HR, suggesting that the *hrc/hrp* gene cluster present is generally incomplete and insufficient for the production of an operational T3SS machinery [58]. Thus, little is known about the architecture of the T3SS carried by *P. fluorescens* strains other than *P. fluorescens* 2P24 [90]. This strain has a filament of more than 1 μm in length, with a diameter of about 13 nm, at the end of there is a basal body composed of two rings, each about 20 nm across. Unfortunately, in one study in which the T3SS machinery was extracted from *P. fluorescens* 2P24 cells by CsCl gradient centrifugation, it was not possible to determine the site of insertion of the T3SS into the cell body [90]. The existence of a functional T3SS in strain C7R12 has been demonstrated, but this machinery was not observed directly [35]. In our assay conditions, TEM provided direct visual evidence of the existence in this strain of a complete T3SS machinery similar to that of Hrp1-T3SS from *P. syringae* and *P. fluorescens* 2P24 [42,53,61,90]. This assertion is based on the typical architecture, size and localization of the putative T3SS detected and because this appendage is observed in the C7R12 strain but not in the C7SM7 mutant, under the same assay conditions (**Fig 4**). It would be interesting in a further study to work on the labeling of proteins characteristic of the extracellular part of T3SS such as HrcC, HrpA or HrpZ to reinforce the characterization of this appendage and better study its role in the interactions between the bacterium and its environment.

The putative T3SS of *P. fluorescens* C7R12 was observed only during culture in an *hrp*-inducting minimal medium in the presence of fructose, which has been reported to be necessary for the observation of the T3SS in *P. syringae* strains [42,53,61], or in the presence of trehalose. We first checked the expression of the *hrp*A gene, as a master controller of T3SS gene expression, in HIM supplemented with mono- (glucose, fructose) or disaccharides (sucrose, trehalose). Interestingly, trehalose was the strongest and earliest inducer of *hrp*A gene expression (**Fig 3**), a finding never before reported, to our knowledge. This compound is a nonreducing sugar found in many organisms, including fungi and plants. In plants, the activated form of the molecule (trehalose-6-phosphate) is a key signal molecule that regulates carbon assimilation and sugar status [95–97]. For fungi, including plant-associated mycorrhizae, trehalose is both a high-energy compound and can be used for glucose storage and osmotic regulation, these tradeoffs favoring its preferential use. It can account for as much as 20% of fungal biomass [98–100]. The presence of trehalose in the environment may alert strain C7R12 cells to the presence of target host-plant or fungal cell, triggering the production of T3SS. This is

consistent with (*i*) the involvement of the T3SS in promoting arbuscular mycorrhization by C7R12 [35], and (*ii*) more generally, the assimilation of trehalose as a substrate by fluorescent pseudomonad populations associated with the rhizosphere and mycorrhizosphere, but not by pseudomonad populations isolated from bare soil [9,101,102]. It has been previously shown that populations of fluorescent pseudomonads harboring T3SS genes were more abundant in mycorrhizospheres than in other environments [27, 59, 62]. Moreover, it has been demonstrated that the T3SS of the strain C7R12 was responsible for the promotion of mycorrhization of *Medicago truncatula* because root colonization by arbuscular mycorrhizal fungi was not promoted by a T3SS-negative mutant [35]. These findings are in agreement with our results.

When *P. fluorescens* C7R12 or C7SM7 was cultured on EM grids containing HIM, the bacteria adhering to the formvar surface formed microcolonies characterized by long, filamentous fibrils composed of bundles of individual pilus strands. These fibrils appeared to be synthesized in a disordered manner close to the bacterium or microcolony (**Fig 5**), subsequently becoming organized and joining together to form long branched bundles up to 50 times the size of the bacteria in our test conditions (**Fig 6**). These structures strikingly resembled the bundles of fimbrial low-molecular-weight protein (Flp) pili first observed by Kachlany et al. [103,104] in *Aggregatibacter* (formerly *Actinobacillus*) *actinomycetemcomitans*, the causal agent of aggressive periodontitis. The other available data suggest that these proteinaceous appendages are related to structures referred to by different authors as the "tight adherence pilus" (Tad) or "rough colony protein" (Rcp) in addition to Flp [105]. The *tad* genes encode the machinery required for the assembly of adhesive Flp pili, including their major structural glycoprotein component, which is encoded by the *flp-1* gene [106]. They are essential for biofilm formation, colonization and pathogenesis in the genera *Aggregatibacter*, *Haemophilus*, *Pasteurella*, *Yersinia*, *Caulobacter* and among the fluorescent pseudomonads of the species *Pseudomonas aeruginosa* (for review see Tomich et al. [107]). Interestingly, *tad* genes have also be implicated in the plant pathogenicity of two potato pathogens, *Pectobacterium* and *Ralstonia* [108,109]. However, among published TEM studies of Flp structures [109–111], images only of Flp fibrils from *A. actinomycetemcomitans* [104,106], and, to a lesser extent, *Ralstonia solanacearum* [112], revealing the structure and size of these fibrils to be similar to those recorded for *P. fluorescens* C7R12 and C7SM7 (**Fig 6**). Bhattacharjee et al. [113], concluded that Flp fibrils were not involved in mobility because they are devoid of the PilT ATPase essential for pilus retraction phenomena, as observed in twitching motility [114]. This is probably also the case for the C7R12 and C7SM7 strains, which displayed no motility in twitching conditions, including culture in HIM, but, conversely, displayed an adhesion of colonies to the surface of Petri dishes (**Fig 1**). By contrast, Flp fibrils contribute to the non-specific adhesion of bacteria to abiotic surfaces (glass, stainless steel) or eukaryotic (mammalian) cells, and they promote bacterial aggregation for the formation of microcolonies and virulence [104–106]. *P. fluorescens* pili clearly act not only in parallel arrays to form thick fibrils, but also in adhesion to environmental surfaces (**Fig 6**). Precisely, the synthesis and assembly of both flagella and Flp pili have recently been shown to be key determinants of plant root colonization [23].

In conclusion, our study provides direct evidence for the existence, in *P. fluorescens* C7R12, of an extracellular apparatus unusual in non-pathogenic fluorescent pseudomonads. This apparatus includes a bundle of polar flagella, thin flexible pili resembling Hrp1-T3SS injectisomes and densely bundled fimbria-like appendages protruding from the entire surface of the microcolony to form a wide fractal network, strongly suspected to support preliminary steps in *Pseudomonas* biofilm deployment. The nature and anchoring of these structures depend on the composition (e.g. sugars), hydrophobicity and density of the cellular microenvironment. Further studies are required to determine the precise role of these various appendages and to check for their existence in other rhizosphere-competent and biocontrol strains.

Supporting information

S1 Table. Primers used for RT-qPCR assays. Underlined sequence of primers used both for 16SrRNA and *hrp*A RT-qPCR assays.
(PDF)

Acknowledgments

We thank members of the *Plateforme de PRotéomique et d'IMAgerie CEllulaire de Normandie* (PRIMACEN, Université de Rouen Normandie) and the *Centre de Microscopie Appliquée à la biologie* (CMAbio, Université de Caen Normandie) to hosting our transmission electron microscopy studies. We also thank Alex Edelman & Associates for linguistic support and Dr. Yoan Konto-Ghiorghi for his help in processing data.

Author Contributions

Conceptualization: Dorian Bergeau, Sylvie Mazurier, Maïté Vicré, Xavier Latour.

Formal analysis: Dorian Bergeau, Sylvie Mazurier, Maïté Vicré, Xavier Latour.

Funding acquisition: Azeddine Driouich, Maïté Vicré, Xavier Latour.

Investigation: Dorian Bergeau, Corinne Barbey, Andrea Chane, Didier Goux, Sophie Bernard, Maïté Vicré.

Methodology: Dorian Bergeau, Sylvie Mazurier, Corinne Barbey, Annabelle Merieau, Didier Goux, Sophie Bernard, Maïté Vicré.

Project administration: Philippe Lemanceau, Maïté Vicré, Xavier Latour.

Supervision: Sylvie Mazurier, Maïté Vicré, Xavier Latour.

Validation: Maïté Vicré, Xavier Latour.

Visualization: Sylvie Mazurier, Maïté Vicré, Xavier Latour.

Writing – original draft: Dorian Bergeau, Xavier Latour.

Writing – review & editing: Sylvie Mazurier, Corinne Barbey, Annabelle Merieau, Didier Goux, Sophie Bernard, Azeddine Driouich, Philippe Lemanceau, Maïté Vicré, Xavier Latour.

References

1. Meyer JM, Geoffroy VA, Baida N, Gardan L, Izard D., Lemanceau P, et al. Siderophore typing, a powerful tool for the identification of fluorescent and nonfluorescent pseudomonads. 2002; 68: 2745–2753. https://doi.org/10.1128/AEM.68.6.2745-2753.2002 PMID: 12039729
2. Bossis E, Lemanceau P, Latour X, Gardan L. The taxonomy of *Pseudomonas fluorescens* and *Pseudomonas putida*: current status and need for revision. Agron Sustain Dev. 2000; 20: 51–63.
3. Palleroni NJ. Introduction to the family *Pseudomonadaceae*, 3071–3085. In A Balows, HG Trüper, M Dworkin, W Harder, KH Schleifer (eds). The prokaryotes. 1992; pp. 3071–3085. 2d edition Springer Verlag, New-York.
4. Palleroni NJ. Human and animal-pathogenic pseudomonads. In edBalows A, Trüper HG, Dworkin M, Harder W, Schleifer KH (eds). The prokaryotes. 1992; pp. 3086–3103. 2d edition Springer Verlag, New-York.
5. Silby MW, Cerdeno-Tarraga AM, Vernikos GS, Giddens SR, Jackson RW, Preston GM, et al. Genomic and genetic analyses of diversity and plant interactions of *Pseudomonas fluorescens*. Genome Biol. 2009; 10: R51. https://doi.org/10.1186/gb-2009-10-5-r51 PMID: 19432983

6. Spiers AJ, Buckling A, Rainey PB. The causes of *Pseudomonas* diversity. Microbiology. 2000; 146: 2345–2350. https://doi.org/10.1099/00221287-146-10-2345 PMID: 11021911
7. Bergsma-Valmi M, Prins ME, Raaijmakers JM. Influence of plant species on population dynamics, genotypic diversity and antibiotic production in the rhizosphere by indigenous *Pseudomonas* spp. FEMS Microbiol Ecol. 2005; 52: 59–69. https://doi.org/10.1016/j.femsec.2004.10.007 PMID: 16329893
8. Bowen GD, Rovira AD. Microbial colonization of plant roots. Annu Rev Phytopathol. 1976; 14: 121–144.
9. Lemanceau P, Corberand T, Gardan L, Latour X, Laguerre G, Boeufgras JM, Alabouvette C. Effect of two plant species (*Linum usitatissinum* L., *Lycopersicon esculentum* Mill.) on the diversity of soil populations of fluorescent pseudomonads. Appl Environ Microbiol. 1995; 61: 1004–1012. PMID: 16534950
10. Silby MW, Winstanley C, Godfrey SAC, Levy SB, Jackson RW. *Pseudomonas* genomes: diverse and adaptable. FEMS Microbiol Rev. 2011; 35: 652–680. https://doi.org/10.1111/j.1574-6976.2011.00269.x PMID: 21361996
11. Diallo S, Crépin A, Barbey C, Orange N, Burini JF, Latour X. Mechanisms and recent advances in biological control mediated through the potato rhizosphere. FEMS Microbiol Ecol. 2011; 75: 351–364. https://doi.org/10.1111/j.1574-6941.2010.01023.x PMID: 21204870
12. Dowling DN O'Gara F. Metabolites of *Pseudomonas* involved in the biocontrol of plant disease. Trends Biotechnol. 1994; 12: 133–140.
13. Haas D, Defago G. Biological control of soil-borne pathogens by fluorescent pseudomonads. Nat Rev Microbiol. 2005; 3: 307–319. https://doi.org/10.1038/nrmicro1129 PMID: 15759041
14. Weller DM. *Pseudomonas* biocontrol agents of soilborne pathogens: looking back over 30 years. Phytopathology. 2007; 97: 250–256. https://doi.org/10.1094/PHYTO-97-2-0250 PMID: 18944383
15. Weston DJ, Pelletier DA, Morell-Falvey JL, Tschaplinski TJ, Jawdy SS, Lu TYL, et al. *Pseudomonas fluorescens* induces strain-dependent and strain-independent host plant responses in defense networks, primary metabolism, photosynthesis, and fitness. Mol Plant-Microbe Interact. 2012; 25: 765–778. https://doi.org/10.1094/MPMI-09-11-0253 PMID: 22375709
16. Fravel DR. Commercialization and implementation of biocontrol. Annu Rev Phytopathol. 2005; 43: 337–359. https://doi.org/10.1146/annurev.phyto.43.032904.092924 PMID: 16078888
17. Ryan PR, Dessaux Y, Thomashow LS, Weller DM. Rhizosphere engineering and management for sustainable agriculture. Plant Soil. 2009; 321: 363–383.
18. Backer R, Rokem JS, Ilangumaran G, Lamont J, Praslickova D, Ricci E, et al. Plant growth-promoting rhizobacteria: context, mechanisms of action, and roadmap to commercialization of biostimulants for sustainable agriculture. Front Plant Sci. 2018; 9: 1473. https://doi.org/10.3389/fpls.2018.01473 PMID: 30405652
19. Barahona E, Navazo A, Martínez-Granero F, Zea-Bonilla T, Perez-Jimenez RM, Martín M, Rivilla R. *Pseudomonas fluorescens* F113 mutant with enhanced competitive colonization ability and improved biocontrol activity against fungal root pathogens. Appl Environ Microbiol. 2011; 77: 5412–5419. https://doi.org/10.1128/AEM.00320-11 PMID: 21685161
20. De Weert S, Bloemberg GV 2007. Rhizosphere competence and the role of root colonization in biocontrol. In Gnanamanickam SS(eds). Plant-associated bacteria. 2007; pp. 317–333. Springer, Dordrecht.
21. Latour X, Delorme S, Mirleau P, Lemanceau P. Identification of traits implicated in the rhizosphere competence of fluorescent pseudomonads: description of a strategy based on population and model strain studies. Agron Sustain Dev (formerly Agronomie). 2003; 23: 397–405.
22. Lugtenberg BJJ, Dekkers L, Bloemberg GV. Molecular determinants of rhizosphere colonization by *Pseudomonas*. Annu Rev Phytopathol. 2001; 39: 461–490. https://doi.org/10.1146/annurev.phyto.39.1.461 PMID: 11701873
23. Cole BJ, Feltcher ME, Waters RJ, Wetmore KM, Mucyn TS, Ryan EM, et al. Genome-wide identification of bacterial plant colonization genes. PLoS Biol. 2017; 15: e2002860. https://doi.org/10.1371/journal.pbio.2002860 PMID: 28938018
24. Conrad JC, Gibiansky ML, Jin F, Gordon VD, Motto DA, Mathewson MA, et al. Flagella and pili-mediated near-surface single-cell motility mechanisms in *Pseudomonas aeruginosa*. Biophys J. 2011; 100: 1608–1616. https://doi.org/10.1016/j.bpj.2011.02.020 PMID: 21463573
25. Haiko J, Westerlund-Wikström B. The role of the bacterial flagellum in adhesion and virulence. Biology (Basel). 2013; 2: 1242–1267.
26. Tseng TT, Tyler BM, Setubal JC. Protein secretion systems in bacterial-host associations, and their description in the gene ontology. BMC Microbiol. 2009; 9: Suppl 1, S2.
27. Viollet A, Corberand T, Mougel C, Robin A, Lemanceau P, Mazurier S. Fluorescent pseudomonads harboring type III secretion genes are enriched in the mycorrhizosphere of *Medicago truncatula*.

FEMS Microbiol Ecol. 2011; 75: 457–467. https://doi.org/10.1111/j.1574-6941.2010.01021.x PMID: 21204867

28. Köhler T, Curty LK, Barja F, Van Delden C, Pechère JC. Swarming of *Pseudomonas aeruginosa* is dependent on cell-to-cell signaling and requires flagella and pili. J Bacteriol. 2000; 182: 5990–5996. https://doi.org/10.1128/jb.182.21.5990-5996.2000 PMID: 11029417

29. Crabill E, Joe A, Block A, van Rooyen JM, Alfano JR. Plant immunity directly or indirectly restricts the injection of type III effectors by the *Pseudomonas syringae* type III secretion system. Plant Physiol. 2010; 154: 233–244. https://doi.org/10.1104/pp.110.159723 PMID: 20624999

30. Jin Q, He SY. Role of the Hrp pilus in type III protein secretion in *Pseudomonas syringae*. Science. 2001; 294: 2556–2558. https://doi.org/10.1126/science.1066397 PMID: 11752577

31. Oh HS, Park DH, Collmer A. Components of the *Pseudomonas syringae* type III secretion system can suppress and may elicit plant innate immunity. Mol Plant-Microbe Interact. 2010; 6: 727–739.

32. Haapalainen M, Van Gestel, Pirhonen M., Taira S. Soluble plant cell signals induce the expression of the type III secretion system of *Pseudomonas syringae* and upregulate the production of pilus protein HrpA. Mol Plant-Microbe Interact. 2009; 22: 282–290. https://doi.org/10.1094/MPMI-22-3-0282 PMID: 19245322

33. Ortiz-Martin I, Thwaites R, Macho AP, Mansfield JW, Beuzon CR. Positive regulation of the Hrp type III secretion system in *Pseudomonas syringae* pv. phaseolicola. Mol Plant-Microbe Interact. 2010; 23: 665–681 https://doi.org/10.1094/MPMI-23-5-0665 PMID: 20367474

34. Mirleau P, Delorme S, Philippot L, Meyer JM, Mazurier S, Lemanceau P. Fitness in soil and rhizosphere of *Pseudomonas fluorescens* C7R12 compared with a C7R12 mutant affected in pyoverdine synthesis and uptake. FEMS Microbiol Ecol. 2000; 34: 35–44. https://doi.org/10.1111/j.1574-6941.2000.tb00752.x PMID: 11053734

35. Viollet A, Pivato B, Mougel C, Cleyet-Marel JC, Gubry-Rangin C, Lemanceau P, Mazurier S. *Pseudomonas fluorescens* C7R12 type III secretion system impacts mycorrhization of *Medicago truncatula* and associated microbial communities. Mycorrhiza. 2017; 27: 23–33. https://doi.org/10.1007/s00572-016-0730-3 PMID: 27549437

36. Fu ZQ, Guo M, Alfano JR. *Pseudomonas syringae* HrpJ is a type III secreted protein that is required for plant pathogenesis, injection of effectors, and secretion of the HrpZ1 harpin. J Bacteriol. 2006; 188: 6060–6069. https://doi.org/10.1128/JB.00718-06 PMID: 16923873

37. King EO, Ward MK, Raney DE. Two simple media for the demonstration of pyocyanin and fluorescin. J Lab Clin Med. 1954; 44: 301–307. PMID: 13184240

38. Huynh T.V., Dahlbeck D., Staskawicz B.J. Bacterial blight of soybean: regulation of a pathogen gene determining host cultivar specificity. Science. 1989; 245: 1374–1377. https://doi.org/10.1126/science.2781284 PMID: 2781284

39. Rossignol G, Merieau A, Guerillon J, Veron W, Lesouhaitier O, Feuilloley MJG, Orange N. Involvement of a phospholipase C in the hemolytic activity of a clinical strain of *Pseudomonas fluorescens*. BMC Microbiol 2008; 8: 189. https://doi.org/10.1186/1471-2180-8-189 PMID: 18973676

40. Bouffartigues E, Moscoso JA, Duchesne R, Rosay T, Fito-Boncompte L, Gicquel G, et al. The absence of the *Pseudomonas aeruginosa* OprF protein leads to increased biofilm formation through variation in c-di-GMP level. Front Microbiol. 2015; 6: 630. https://doi.org/10.3389/fmicb.2015.00630 PMID: 26157434

41. Livak KJ, Schmittgen TD. Analysis of relative gene expression data using real-time quantitative PCR and the 2(-DeltaDelta C(T)) method. Methods San Diego Calif. 2001; 25: 402–408.

42. Roine E, Wei W, Yuan J, Nurmiaho-Lassila EL, Kalkkinen N, Romantschuk M, He SY. Hrp pilus: an hrp-dependent bacterial surface appendage produced by *Pseudomonas syringae* pv. tomato DC3000. Proc Natl Acad Sci USA. 1997; 94: 3459–3464. https://doi.org/10.1073/pnas.94.7.3459 PMID: 9096416

43. Yang A, Tang WS, Si T, Tang JX. Influence of physical effects on the swarming motility of *Pseudomonas aeruginosa*. Biophysical J. 2017; 112: 1462–1471.

44. Deziel E, Comeau Y, Villemur R. Initiation of biofilm formation by *Pseudomonas aeruginosa* 57RP correlates with emergence of hyperpiliated and highly adherent phenotypic variants deficient in swimming, swarming, and twitching motilities. J Bacteriol. 2001; 183: 1195–1204. https://doi.org/10.1128/JB.183.4.1195-1204.2001 PMID: 11157931

45. Kearns DB. A field guide to bacterial swarming motility. Nat Rev Microbiol. 2010; 8: 634–644. https://doi.org/10.1038/nrmicro2405 PMID: 20694026

46. Rossignol G, Sperandio D, Guerillon J, Duclairoir-Poc C, Soum-Soutera E, Orange N, et al. Phenotypic variation in the *Pseudomonas fluorescens* clinical strain MFN1032. Res Microbiol. 2009; 160: 337–344. https://doi.org/10.1016/j.resmic.2009.04.004 PMID: 19409488

47. Rashid MH, Kornberg A. Inorganic polyphosphate is needed for swimming, swarming, and twitching motilities of *Pseudomonas aeruginosa*. Proc Natl Acad Sci USA. 2000; 97: 4885–4890. https://doi.org/10.1073/pnas.060030097 PMID: 10758151

48. Turnbull L., Whitchurch B. Motility assay: twitching motility. Methods Mol Biol. 2014; 1149: 73–86. https://doi.org/10.1007/978-1-4939-0473-0_9 PMID: 24818899

49. Tauschel HD. ATPase activity of the polar organelle demonstrated by cytochemical reaction in whole unstained cells of *Rhodopseudomonas palustris*. Arch Microbiol. 1987; 148: 159–161.

50. Hintsche M, Waljor V, Großmann R, Kühn MJ, Thormann KM, Peruani F, Beta C. A polar bundle of flagella can drive bacterial swimming by pushing, pulling, or coiling around the cell body. Sci Rep. 2017; 7: 16771. https://doi.org/10.1038/s41598-017-16428-9 PMID: 29196650

51. Dasgupta N, Ashare A, Hunninghake GW, Yahr TL. Transcriptional induction of the *Pseudomonas aeruginosa* type III secretion system by low Ca^{2+} and host cell contact proceeds through two distinct signaling pathways. Infect Immun. 2006; 74: 3334–41. https://doi.org/10.1128/IAI.00090-06 PMID: 16714561

52. Geilfus CM. The pH of the apoplast: dynamic factor with functional impact under stress. Mol Plant. 2017; 10: 1371–1386. https://doi.org/10.1016/j.molp.2017.09.018 PMID: 28987886

53. Brown IR, Mansfield JW, Taira S, Roine E, Romantschuk M. Immunocytochemical localization of HrpA and HrpZ supports a role for the Hrp pilus in the transfer of effector proteins from *Pseudomonas syringae* pv. tomato across the host plant cell wall. Mol Plant-Microbe Interact. 2001; 14: 394–404. https://doi.org/10.1094/MPMI.2001.14.3.394 PMID: 11277437

54. Tampakaki AP. Commonalities and differences of T3SSs in rhizobia and plant pathogenic bacteria. Front Plant Sci. 2014; 5: 1–19.

55. Collmer A, Lindeberg M, Petnicki-Ocwieja T, Schneider D, Alfano J. Genomic mining type III secretion system effectors in *Pseudomonas syringae* yields new picks for all TTSS prospectors. Trends Microbiol. 2002; 10: 462–469. PMID: 12377556

56. Greenberg J, Vinatzer BA. Identifying type III effectors of plant pathogens and analyzing their interaction with plant cells. Curr Opin Microbiol. 2003; 6: 20–28. PMID: 12615215

57. Guo M, Tian F, Wamboldt Y, Alfano JR. The majority of the type III effector inventory of *Pseudomonas syringae* pv. tomato DC3000 can suppress plant immunity. Mol Plant-Microbe Interact. 2009; 22: 1069–1080. https://doi.org/10.1094/MPMI-22-9-1069 PMID: 19656042

58. Mazurier S, Merieau A, Bergeau D, Decoin V, Sperandio D, Crépin A, et al. Type III secretion system and virulence markers highlight similarities and differences between human- and plant-associated pseudomonads related to *Pseudomonas fluorescens* and *P. putida*. Appl Environ Microbiol. 2015; 81: 2579–2590. https://doi.org/10.1128/AEM.04160-14 PMID: 25636837

59. Nazir R, Mazurier S, Yang P, Lemanceau P, van Elsas JD. The ecological role of type three secretion systems in the interaction of bacteria with fungi in soil and related habitats is diverse and context-dependent. Front Microbiol. 2017; 8: 38. https://doi.org/10.3389/fmicb.2017.00038 PMID: 28197129

60. Cornelis GR. The type III secretion injectisome. Nature Rev. 2006; 4: 811–825.

61. Li CM, Brown I, Mansfield J, Stevens C, Boureau T, Romantschuk M, Taira S. The Hrp pilus of *Pseudomonas syringae* elongates from its tip and acts as a conduit for translocation of the effector protein HrpZ. EMBO J. 2002; 21: 1909–1915. https://doi.org/10.1093/emboj/21.8.1909 PMID: 11953310

62. Mazurier S, Lemunier M, Siblot S, Mougel C, Lemanceau P. Distribution and diversity of type III secretion system-like genes in saprophytic and phytopathogenic fluorescent pseudomonads. FEMS Microbiol Ecol. 2004; 49: 455–467. https://doi.org/10.1016/j.femsec.2004.04.019 PMID: 19712294

63. Lemanceau P, Alabouvette C. Biological control of Fusarium diseases by fluorescent *Pseudomonas* and non-pathogenic *Fusarium*. Crop Protect. 1991; 10: 279–286.

64. Pivato B, Offre P, Marchelli S, Barbonaglia B, Mougel C, Lemanceau P, Berta G. Bacterial effects on arbuscular mycorrhizal fungi and mycorrhization as influenced by the bacteria, fungi and host-plant. Mycorrhiza. 2009; 19: 81–90. https://doi.org/10.1007/s00572-008-0205-2 PMID: 18941805

65. Sanchez L, Weidmann S, Arnould C, Bernard AR, Gianninazzi S, Gianninazzi-Pearson V. *Pseudomonas fluorescens* and *Glomus mosseae* trigger *DMI3*-dependent activation of genes related to a signal transduction pathway in roots of *Medicago truncatula*. Plant Physiol. 2005; 139: 1065–1077. https://doi.org/10.1104/pp.105.067603 PMID: 16183836

66. Eparvier A, Lemanceau P, Alabouvette C. Population dynamics of non-pathogenic *Fusarium* and fluorescent *Pseudomonas* strains in rockwool, a substratum for soilless culture. FEMS Microbiol Ecol. 1991; 86: 177–184.

67. Ghirardi S, Dessaint F, Mazurier S, Corberand T, Raaijmakers JM, Meyer JM, et al. Identification of traits shared by rhizosphere-competent strains of fluorescent pseudomonads. Microb Ecol. 2012; 64: 725–37. https://doi.org/10.1007/s00248-012-0065-3 PMID: 22576821

68. Mirleau P, Philippot L, Corberand T, Lemanceau P. Involvement of nitrate reductase and pyoverdine in competitiveness of *Pseudomonas fluorescens* strain C7R12 in soil. Appl Environ Microbiol. 2001; 67: 2627–2635. https://doi.org/10.1128/AEM.67.6.2627-2635.2001 PMID: 11375173

69. Shirley M, Avoscan L, Bernaud E, Vansuyt G, Lemanceau P. Comparison of iron acquisition from Fe–pyoverdine by strategy I and strategy II plants. Botany 2011; 89: 731–735.

70. Trapet P, Avoscan L, Klinguer A, Pateyron S, Citerne S, Chervin C, et al. The *Pseudomonas fluorescens* siderophore pyoverdine weakens *Arabidopsis thaliana* defense in favor of growth in iron-deficient conditions. Plant Physiol. 2016; 171: 675–93. https://doi.org/10.1104/pp.15.01537 PMID: 26956666

71. Vansuyt G, Robin A, Briat JF, Curie C, Lemanceau P. Iron acquisition from Fe-pyoverdine by *Arabidopsis thaliana*. Mol Plant-Microbe Interact. 2007; 20: 441–4472007 https://doi.org/10.1094/MPMI-20-4-0441 PMID: 17427814

72. Latour X, Lemanceau P. Carbon and energy metabolism of oxidase-positive saprophytic fluorescent *Pseudomonas* spp. Agron Sustain Dev (formerly Agronomie). 1997; 17: 427–443.

73. Belas R. Biofilms, flagella, and mechanosensing of surfaces by bacteria. Trends Microbiol. 2014; 22: 517–527. https://doi.org/10.1016/j.tim.2014.05.002 PMID: 24894628

74. Berg HC. The rotary motor of bacteria flagella. Annu Rev Biochem. 2003; 72: 19–54. https://doi.org/10.1146/annurev.biochem.72.121801.161737 PMID: 12500982

75. Barahona E, Navazo A, Garrido-Sanz D, Muriel C, Martínez-Granero F, Redondo-Nieto M, et al. *Pseudomonas fluorescens* F113 can produce a second flagellar apparatus, which is important for plant root colonization. Front Microbiol. 2016; 7: 1471. https://doi.org/10.3389/fmicb.2016.01471 PMID: 27713729

76. Ping L, Birkenbeil J, Monajembashi S. Swimming behavior of the monotrichous bacterium *Pseudomonas fluorescens* SBW25. FEMS Microbiol Ecol. 2013; 86: 36–44. https://doi.org/10.1111/1574-6941.12076 PMID: 23346905

77. De Weger LA, van der Vlugt CI, Wijfjes AH, Bakker PA, Schippers B, Lugtenberg B. Flagella of a plant-growth-stimulating *Pseudomonas fluorescens* strain are required for root colonization of potato roots. J Bacteriol. 1987; 169: 2769–2773 https://doi.org/10.1128/jb.169.6.2769-2773.1987 PMID: 3294806

78. Raatz M, Hintsche M, Bahrs M, Theves M, Beta C. Swimming patterns of a polarly flagellated bacterium in environments of increasing complexity. Eur Phys J Special Topics 2015; 224: 1185–1198.

79. Hazelbauer GL, Falke JJ, Parkinson JS. Bacterial chemoreceptors: high-performance signaling in networked arrays. Trends Biochem Sci. 2008; 33: 9–19. https://doi.org/10.1016/j.tibs.2007.09.014 PMID: 18165013

80. Collmer A, Badel JL, Charkowski AO, Deng W-L, Fouts DE, Ramos AR, et al. *Pseudomonas syringae* Hrp type III secretion system and effector proteins. Proc Natl Acad Sci USA. 2000; 97: 8770–8777. https://doi.org/10.1073/pnas.97.16.8770 PMID: 10922033

81. Ramos JL. *Pseudomonas*: virulence and gene regulation. 2004; Vol 2. Kluwer Academic Plenum Publishers, New York, NY.

82. Cornelis GR. The type III secretion injectisome, a complex nano-machine for intracellular "toxin" delivery. Biol Chem. 2010; 391: 745–751. https://doi.org/10.1515/BC.2010.079 PMID: 20482311

83. Loper JE, Hassan KA, Mavrodi DV, Davis II EW, Kent Lim C, Shaffer BT et al. Comparative genomics of plant-associated *Pseudomonas* spp.: insights into diversity and inheritance of traits involved in multitrophic interactions. PLoS Genetics 2012; 8: e1002784. https://doi.org/10.1371/journal.pgen.1002784 PMID: 22792073

84. Troisfontaines P, Cornelis GR. Type III secretion: more systems than you think. Physiology. 2005; 20: 326–339.

85. Engel J, Balachandran P. Role of *Pseudomonas aeruginosa* type III effectors in disease. Curr Opin Microbiol. 2009; 12: 61–66. https://doi.org/10.1016/j.mib.2008.12.007 PMID: 19168385

86. Quinaud M, Chabert J, Faudry E, Neumann E, Lemaire D., Pastor, et al. The PscE-PscF-PscG complex controls type III secretion needle biogenesis in *Pseudomonas aeruginosa*. J Biol Chem. 2005; 280: 36293–36300. https://doi.org/10.1074/jbc.M508089200 PMID: 16115870

87. Dean P. Functional domains and motifs of bacterial type III effector proteins and their roles in infection. FEMS Microbiol Rev. 2011; 35: 1100–1125. https://doi.org/10.1111/j.1574-6976.2011.00271.x PMID: 21517912

88. Barret M, Egan F, Moynihan J, Morrissey JP, Lesouhaitier O, O'Gara F. Characterization of the SPI-1 and Rsp type three secretion systems in *Pseudomonas fluorescens* F113. Environ Microbiol Rep. 2013; 5: 377–386. https://doi.org/10.1111/1758-2229.12039 PMID: 23754718

89. Cusano AM, Burlinson P, Deveau A, Vion P, Uroz S, Preston GM, Frey-Klett P. *Pseudomonas fluorescens* BBc6R8 type III secretion mutants no longer promote ectomycorrhizal symbiosis. Environ Microbiol Rep. 2011; 3: 203–210. https://doi.org/10.1111/j.1758-2229.2010.00209.x PMID: 23761252

90. Liu P, Zhang W, Zhang LQ, Liu X, Wei HL. Supramolecular structure and functional analysis of the type III secretion system in *Pseudomonas fluorescens* 2P24. Front Plant Sci. 2016; 6: 1190. https://doi.org/10.3389/fpls.2015.01190 PMID: 26779224

91. Marchi M, Boutin M, Gazengel K, Rispe C, Gauthier JP, Guillerm-Erckelboudt AY, et al., Genomic analysis of the biocontrol strain *Pseudomonas fluorescens* Pf29Arp with evidence of T3SS and T6SS gene expression on plant roots. Environ Microbiol Rep. 2013; 5: 393–403. https://doi.org/10.1111/1758-2229.12048 PMID: 23754720

92. Mavrodi DV, Joe A, Mavrodi OV, Hassan KA, Weller DM, Paulsen IT, et al. Structural and functional analysis of the type III secretion system from *Pseudomonas fluorescens* Q8r1-96. J Bacteriol. 2011; 193: 177–189. https://doi.org/10.1128/JB.00895-10 PMID: 20971913

93. Preston GM, Bertrand N, Rainey PB. Type III secretion in plant growth-promoting *Pseudomonas fluorescens* SBW25. Mol Microbiol. 2001; 41: 999–1014. https://doi.org/10.1046/j.1365-2958.2001.02560.x PMID: 11555282

94. Rezzonico F, Binder C, Defago G, Moenne-Loccoz Y. The type III secretion system of biocontrol *Pseudomonas fluorescens* KD targets the phytopathogenic *Chromista Pythium ultimum* and promotes cucumber protection. Mol Plant-Microbe Interact. 2005; 18: 991–1001. https://doi.org/10.1094/MPMI-18-0991 PMID: 16167769

95. Paul MJ, Primavesi LF, Jhurreea D, Zhang Y. Trehalose metabolism and signaling. Annu Rev Plant Biol. 2008; 59: 417–441. https://doi.org/10.1146/annurev.arplant.59.032607.092945 PMID: 18257709

96. Ponnu J, Wahl V, Schmid M. Trehalose-6-phosphate: connecting plant metabolism and development. Front Plant Sci. 2011; 2: 70. https://doi.org/10.3389/fpls.2011.00070 PMID: 22639606

97. Poueymiro M, Cazalé AC, François JM, Parrou JL, Peeters N, Genin S. A *Ralstonia solanacearum* type III effector directs the production of the plant signal metabolite trehalose-6-phosphate. mBio. 2014; 5: e02065–14. https://doi.org/10.1128/mBio.02065-14 PMID: 25538193

98. Treseder KK, Lennon JT. Fungal traits that drive ecosystem dynamics on land. Microbiol Mol Biol Rev. 2015; 79: 243–262. https://doi.org/10.1128/MMBR.00001-15 PMID: 25971588

99. Van Laere A. Trehalose, reserve and/or stress metabolite? FEMS Microbiol Rev. 1989; 63: 201–210.

100. Wiemken V. Trehalose synthesis in ectomycorrhizas–a driving force of carbon gain for fungi? New Phytol. 2007; 17: 228–230.

101. Frey P, Frey-Klett P, Garbaye J, Berge O, Heulin T. Metabolic and genotypic fingerprinting of fluorescent pseudomonads associated with the Douglas Fir-*Laccaria bicolor* mycorrhizosphere. Appl Environ Microbiol. 1997; 63: 1852–1860 PMID: 16535600

102. Latour X, Corberand T, Laguerre, Allard F., Lemanceau P. The composition of fluorescent pseudomonad populations associated with roots is influenced by plant and soil type. Appl Environ Microbiol. 1996; 62: 2449–2456. PMID: 16535355

103. Kachlany SC, Planet PJ, Bhattacharjee MK, Kollia E, DeSalle R, Fine DH, Figurski DH. Nonspecific adherence by *Actinobacillus actinomycetemcomitans* requires genes widespread in bacteria and archaea. J Bacteriol. 2000; 182: 6169–6176. https://doi.org/10.1128/jb.182.21.6169-6176.2000 PMID: 11029439

104. Kachlany SC., Planet PJ, Desalle R, Fine DH, Figurski DH. Genes for tight adherence of *Actinobacillus actinomycetemcomitans*: from plaque to plague to pond scum. Trends Microbiol. 2001; 9: 429–37. PMID: 11553455

105. Berry JL, Pelicic V. Exceptionally widespread nanomachines composed of type IV pilins: the prokaryotic swiss army knives. FEMS Microbiol Rev. 2015; 39: 134–154. https://doi.org/10.1093/femsre/fuu001 PMID: 25793961

106. Kachlany SC., Planet PJ, Desalle R, Fine DH, Figurski DH, Kaplan JB. *flp-1*, the first representative of a new pilin gene subfamily, is required for non-specific adherence of *Actinobacillus actinomycetemcomitans*. Mol Microbiol. 2001; 40: 542–54. https://doi.org/10.1046/j.1365-2958.2001.02422.x PMID: 11359562

107. Tomich M, Planet PJ, Figurski DH. The *tad* locus: postcards from the widespread colonization island. Nat Rev Microbiol. 2007; 5: 363–375. https://doi.org/10.1038/nrmicro1636 PMID: 17435791

108. Nykyri J, Mattinen L, Niemi O, Adhikari S, Kõiv V, Somervuo P, et al. Role and regulation of the Flp/Tad pilus in the virulence of *Pectobacterium atrosepticum* SCRI1043 and *Pectobacterium wasabiae* SCC3193. PLoS One. 2013; 8: e73718. https://doi.org/10.1371/journal.pone.0073718 PMID: 24040039

109. Wairuri CK, Van Der Waals JE, Van Schalkwyk A, Theron J. *Ralstonia solanacearum* needs Flp pili for virulence on potato. Mol Plant-Microbe Interact. 2012; 25: 546–56. https://doi.org/10.1094/MPMI-06-11-0166 PMID: 22168446

110. Bernard CS, Bordi C, Termine E, Filloux A, De Bentzmann S. Organization and PprB-dependent control of the *Pseudomonas aeruginosa* tad locus, involved in Flp pilus biology. J Bacteriol. 2009; 191: 1961–1973 https://doi.org/10.1128/JB.01330-08 PMID: 19151143

111. Boyd JM, Dacanay A, Knickle LC, Touhami A, Brown LL, Jericho MH, et al. Contribution of type IV pili to the virulence of *Aeromonas salmonicida* subsp. *salmonicida* in Atlantic salmon (*Salmo salar* L.). Infect Immun. 2008; 76: 1445–55. https://doi.org/10.1128/IAI.01019-07 PMID: 18212071

112. Van Gijsegem F, Vasse J, Camus JC, Marenda M, Boucher C. *Ralstonia solanacearum* produces hrp-dependent pili that are required for PopA secretion but not for attachment of bacteria to plant cells. Mol Microbiol. 2000; 36: 249–60. https://doi.org/10.1046/j.1365-2958.2000.01851.x PMID: 10792714

113. Bhattacharjee MK, Kachlany SC, Fine DH, Figurski DH. Nonspecific adherence and fibril biogenesis by *Actinobacillus actinomycetemcomitans*: TadA protein is an ATPase. J Bacteriol. 2001; 183: 5927–5936. https://doi.org/10.1128/JB.183.20.5927-5936.2001 PMID: 11566992

114. Burrows LL. *Pseudomonas aeruginosa* twitching motility: type IV pili in action. Annu Rev Microbiol. 2012; 66: 493–520. https://doi.org/10.1146/annurev-micro-092611-150055 PMID: 22746331